Solid Geometric Object Reconstruction from Single Line Drawing Image

Jinxin Zheng, Yongtao Wang[*] and Zhi Tang
Institute of Computer Science and Technology, Peking University,
No.5 Yiheyuan Road, Haidian District, 100871 Beijing, China

Keywords: 3D Reconstruction, Line Drawing, Sketch Extraction.

Abstract: We present a robust method to reconstruct solid geometric object from single line drawing image taken from the geometric books. Unlike most of the existing methods which require perfect and complete sketches of the line drawings as the inputs, our method directly takes the line drawing images as the inputs and can well handle the incomplete sketches that are automatically produced by our sketch extraction algorithm. The proposed method consists of three major steps as follows: First, the sketch of the input line drawing (i.e., line segments and their intersections) is automatically extracted and further represented as an undirected graph. Second, candidate 3D models from the pre-built 3D model database are found by graph matching. Third, for each candidate 3D model, the model parameters, the rotation and the translation aligning the model with the sketch, are found by optimizing an objective function which is composed of the residuals between the vertices of the sketch and the 2D projections of the candidate model's vertices, and an optimal reconstruction solution is further selected as the final result. Experimental results show that our method can effectively reconstruct the solid geometric object from single line drawing image.

1 INTRODUCTION

Many publications often contain a large amount of illustrations of the solid geometric objects, such as geometry and engineering textbooks. These illustrations consisting of several line segments or arcs are called line drawings. Moreover, such kind of illustrations, which are actually the parallel projections of the corresponding solid geometric objects, are usually manufactured in a two-dimensional (2D) way and stored as 2D line drawing images. Hence, the three-dimensional (3D) information of the corresponding solid geometric objects is not contained in the electronic documents of those publications.

In this mobile era, more and more people start reading and learning on their mobile devices such as tablet PCs and cell phones. Furthermore, the mobile devices now have been powerful enough to render 3D geometric objects in real time. Therefore, as illustrated in Figure 1, if we can restore the 3D structure of those solid geometric objects from the corresponding 2D line drawing images, we can present the illustrations of them in a 3D style on the mobile devices, and thereby can significantly improve the users' reading and learning experience.

[*]Corresponding author. Telephone: +86 010 82529542 Fax: +86 010 62754532

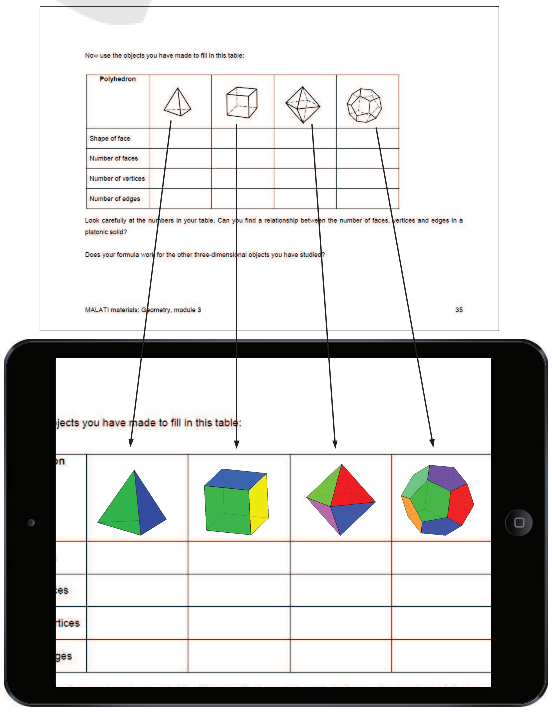

Now use the objects you have made to fill in this table:

Polyhedron				
Shape of face				
Number of faces				
Number of vertices				
Number of edges				

Look carefully at the numbers in your table. Can you find a relationship between the number of faces, vertices and edges in a platonic solid?

Does your formula work for the other three-dimensional objects you have studied?

MALATI materials: Geometry, module 3 35

Figure 1: Illustration of the application of solid geometric object reconstruction technology to mobile reading. The solid objects from left to right are tetrahedron, cube, octahedron and dodecahedron respectively.

Zheng J., Wang Y. and Tang Z..
Solid Geometric Object Reconstruction from Single Line Drawing Image.
DOI: 10.5220/0005261203910400
In *Proceedings of the 10th International Conference on Computer Graphics Theory and Applications* (GRAPP-2015), pages 391-400
ISBN: 978-989-758-087-1
Copyright © 2015 SCITEPRESS (Science and Technology Publications, Lda.)

The human can easily obtain the 3D structural information of an object from a single 2D line drawing image, but how to make a computer have the same ability remains a challenging problem. Over decades, a number of methods have been proposed to reconstruct the 3D geometric objects from single line drawings. However, to the best of our knowledge, all these methods assume that the input is the perfect sketch of the line drawings, that is, all the line segments and their intersections are correctly obtained. Therefore, in this perspective, these methods are not capable of achieving the task addressed in this paper, which is the solid geometric object reconstruction from single line drawing image. The main reason is that, the sketch automatically extracted from single line drawing image may be inaccurate, due to the limitations of the algorithms involved in the sketch extraction process or the poor quality of the line drawing image. Hence, we need to find a more robust reconstruction method, which can handle incomplete or inaccurate sketches.

The key contribution of our work is an algorithm to reconstruct 3D geometric objects from single line drawing images. Compared to the existing methods, the proposed method is able to handle inaccurate sketches which are not demonstrated in any previous works. Based on this algorithm, we implement a mobile application which allows the user to tap on the line drawing images in the screen of the phone or tablet, then it instantly reconstructs the geometric object in the image, and draws the reconstructed 3D object onto the screen. The user can interact with the 3D object by gestures including dragging and rotating, which is essential to improve the user experience in reading such electronic materials.

The rest of this paper is organized as follows. The related work is briefly reviewed in section 2. An overview and some assumptions of our method are provided in section 3. Section 4 mainly discusses the sketch extraction process in our method. Section 5 describes the 3D model matching process. Section 6 presents the 3D reconstruction algorithm. Experimental results are provided in section 7 and conclusions are drawn in section 8.

2 RELATED WORK

In the past two decades, a lot of researchers made efforts to resolve the single line drawing-based 3D reconstruction problem. These methods can be roughly categorized into 3 types: the regularity-based methods, the deduction-based methods and the divide-and-conquer-based methods.

Regularity-based methods use some geometric rules as constraints to construct a cost function, and then minimize this function to obtain the 3D object. Conventional rules include: (1) the face planarity rule: the coplanar vertices of the line drawing should also be coplanar 3D points after reconstruction (Leclerc and Fischler, 1992; Shpitalni and Lipson, 1996; Liu and Lee, 2001; Liu et al., 2002; Liu and Tang, 2005); (2) angularity rule: all the angles at the vertices of a line drawing should be the same (Marill, 1991; Brown and Wang, 1996; Shoji et al., 2001). Besides the preceding two rules, Lipson and Shpitalni(Lipson and Shpitalni, 1996) propose another 10 rules, such as line parallelism, line verticality, isometry and corner orthogonality, et al. Since the dimension of the search space according to this type of methods is very high, some works (Liu et al., 2008; Tian et al., 2009) try to reduce the dimension of the search space to improve the computational efficiency of these methods.

Deduction-based methods usually make stronger assumptions over the 3D objects corresponding to the input line drawings, e.g., the 3D object has cubic corners (Lee and Fang, 2011; Lee and Fang, 2012), or a symmetric plane exists in the 3D object (Cordier et al., 2013), and so on. Based on these assumptions, the reconstruction result is obtained by a deduction process.

The third type of methods adopt divide-and-conquer strategy to reconstruct the complex line drawings (Chen et al., 2007; Xue et al., 2010; Liu et al., 2011; Zou et al., 2014b; Yang et al., 2013; Zou et al., 2014a; Xue et al., 2012). These methods split the line drawing to a set of simpler parts. In particular, the traditional regularity-based methods are often used to reconstruct each part. Among these methods, Xue et al. (Xue et al., 2012) propose a refined divide-and-conquer-based method, in which an example-based approach is used to reconstruct each part of the complex line drawing.

Given the perfect sketch of the line drawings as the input, the above methods achieve good reconstruction results. However, none of them demonstrate their abilities to handle inaccurate sketches. In this work, we present a more robust method to solve the single line drawing-based 3D reconstruction problem, which can handle inaccurate sketches. It worths noting that our method is example-based, the same as the Xue et al (Xue et al., 2012)'s method (E3D). The main differences between our method and E3D are twofold: 1. The E3D method can only take the sketch of a line drawing as input, while our method directly takes line drawing image as input; 2. The E3D method needs complete input sketches without missing or erroneous

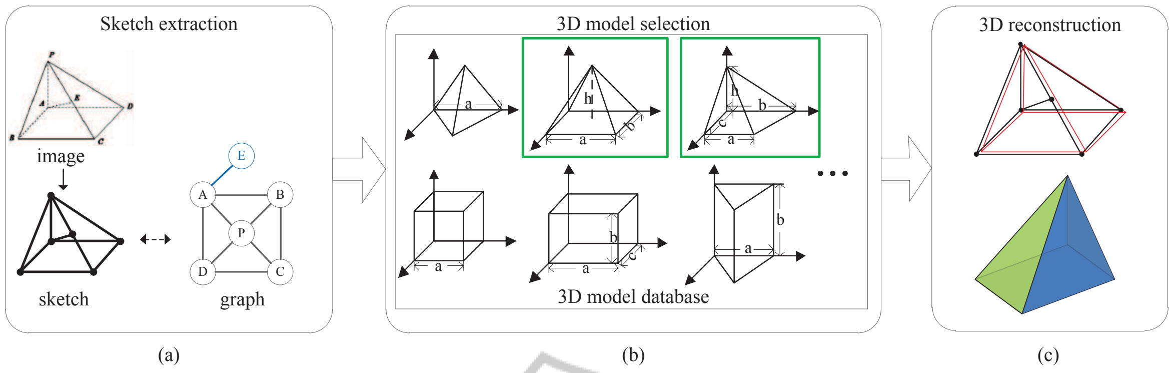

Figure 2: A brief illustration of our method. (a) Sketch extraction: the sketch is extracted by detecting the line segments and intersections from the input line drawing image, and is represented by an undirected connected graph. (b) 3D model selection: candidate 3D models (marked in green bounds) are selected from the 3D model database based on sub-graph isomorphism. (c) 3D reconstruction: the reconstruction result is obtained by fitting the candidate models (red lines) to the sketch (black lines). The reconstructed solid geometric object (a pyramid) is shown from another point of view.

edges, while our method does not need that. Although the E3D method can handle more complex objects based on a divide-and-conquer approach, it requires the input to be a complete sketch of the line drawing. Actually, all the experimental data shown in E3D is man-made sketches created from a CAD software, while our input data is the geometric images from the PDF documents. Experimental results demonstrate that our method is able to produce good results for inaccurate sketches automatically extracted from the input line drawing images.

3 OVERVIEW

Our method has three main steps. First, we extract the lines from the image and convert them to an undirected connected graph, which is called the sketch. Note that due to the limitation of the sketch extraction algorithm, the extracted sketch is highly possible to be inaccurate or even incomplete. Second, the extracted sketch is matched within a pre-built 3D model database, producing some candidate models that are analog to the sketch. Finally, an objective function is constructed based on the coordinate residuals between the graph and the candidate models, and then an optimal reconstruction solution is found based on an optimization selection process. A brief illustration of our algorithm is shown in Figure 2. It is worth noting that, in this paper, we only consider the line drawings solely consisting of straight line segments, since most of the illustrations fall into this category. The line drawings containing arcs will be considered in our future work.

In order to clearly present our solution to the single line drawing-base 3D reconstruction problem, we first fix the related notations and definitions.

Definition 1. *A* **2D sketch** *is the graph representation of the line drawing image, denoted by $S = (\mathbf{x}, G_s)$, where $\mathbf{x} = \{x_1, x_2, \ldots, x_n\}$ are the 2D coordinates of the vertices, and G_s is the undirected connected graph indicating which two vertices are connected.*

Definition 2. *A* **3D object** *is represented as an undirected connected graph in 3D space, that is, $O = (\mathbf{X}, G_o)$, where $\mathbf{X} = \{X_1, X_2, \ldots, X_m\}$ are the 3D coordinates of the vertices of the object, and G_o is the undirected connected graph indicating which two vertices are connected.*

Definition 3. *A* **3D model** *represents a kind of 3D object controlled by a set of model parameters, which is denoted by $M = (\mathbf{A}, \mathbf{X}, G_m)$, where $\mathbf{A}$ is the set of parameters, $\mathbf{X}$ is the set of vertices, and G_m is the undirected connected graph indicating which two vertices are connected.*

Definition 4. *An* **instance of the 3D model** *is an 3D object that is generated by the rotation and translation of the 3D model in 3D space.*

4 SKETCH EXTRACTION

The input gray-scale image (the color image is first converted to the gray-scale one) is scaled to a normal size(the longer edge is sized to 400 pixels and the shorter edge is sized into corresponding proportion), and then binarized with the OTSU method (Otsu, 1975), and then connected components of the foreground pixels (the black pixels of the original input image) are obtained.

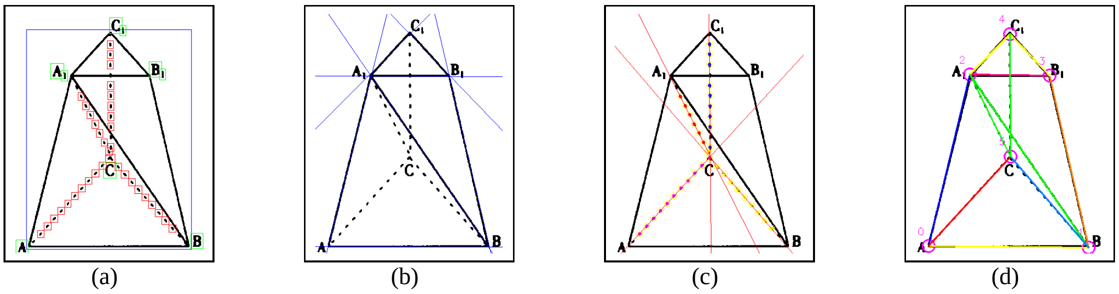

Figure 3: Illustration of sketch extraction. (a) connected component clustering. (b) solid line extraction. (c) dashed line extraction. (d) generating the sketch (undirected connected graph).

4.1 Connected Component Clustering

As shown in Figure 3(a), there are usually 3 types of the connected components according to their sizes: the main body (the one bounded in blue rectangle), the dashed line dots (the ones in red rectangles), and the characters (the ones in green rectangles). Based on these observations, We adopt the k-means (Hartigan and Wong, 1979) clustering (we set k=3 straightforwardly) algorithm to classify the types of the connected components. The count of the foreground pixels, the height and width of the bounding box are taken as the feature for clustering. After clustering, we divide the connected components into 3 types: the one whose bounding box is significantly larger than the others is selected as the main body; the ones with smallest bounding boxes and similar foreground pixel counts are classified to the dashed line dots; the remaining ones are then classified to the characters, which are not involved in our further processing. This strategy is simple yet effective to provide an estimation of the component types.

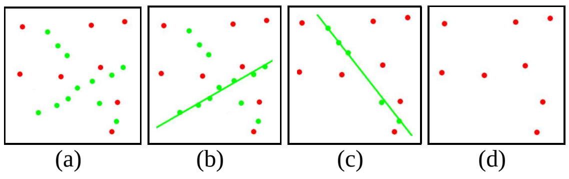

Figure 4: The consensus-sampling extraction process (a) the inliers and the outliers. (b)(c) lines extracted by consensus-sampling of the inliers. (d) left outliers.

4.2 Line Extraction

We use the edge segment-based (Liu et al., 2014) to extract the solid lines(Figure 3(b)), and propose a sample-consensus-based algorithm (summarized in algorithm 1) for dashed line extraction. The dashed dots are first shrink to their center points as the input of the algorithm. The dashed line extraction process is illustrated in Figure 4. Figure 4(a) shows all the input center points: the inliers are marked in green color and the outliers are in red. Then two lines are sequentially extracted by the sample-consensus process in Figure 4(b) and 4(c), after which only outlier points are left in Figure 4(d). This algorithm is efficient and robust in presence of a few outliers. Figure 3(c) shows an example of the extracted dashed lines from the line drawing image.

Algorithm 1: Dashed line extraction.

```
Input:
    A set of central points $\mathbf{V} = \{v_1, v_2, \ldots, v_n\}$;
Output:
    A set of lines $\mathbf{L}$;
1: $\mathbf{L} = \phi, \mathbf{G} = \phi$;
2: For each pair of points $v_i, v_j \in \mathbf{V}$, calculate the
   line $l_{ij}$ that goes through them, and find the inlier
   points set $\mathbf{P}_{ij}$. Add $\mathbf{P}_{ij}$ to $\mathbf{G}$;
3: while $\mathbf{G}$ is not empty do
4:     $\mathbf{P} := \arg\max |\mathbf{P}_{ij}|, i, j \in [1, n]$. If $|\mathbf{P}| < 3$ output
       $\mathbf{L}$ and exit.
5:     Calculate the line $l$ by least-squares fitting of
       the points in $\mathbf{P}$.
6:     Add $l$ to set $\mathbf{L}$. Remove $\mathbf{P}$ from $\mathbf{G}$. Remove
       all the points in $\mathbf{P}$ from the set $\mathbf{V}$, and from all
       existing $\mathbf{P}_{ij}$ sets in $\mathbf{G}$.
7: end while
8: Output $\mathbf{L}$ and stop.
```

4.3 Generating the Sketch

After the solid and dashed lines are extracted from the input image, we further convert them into an undirected connected graph. First, the intersection points of the lines are determined, and the lines are cut into line segments according to these intersection points. Second, an image-based validation process is performed to remove the false segments that only cover very few foreground pixels. Third, the line segments that are adjacent and collinear are merged to one seg-

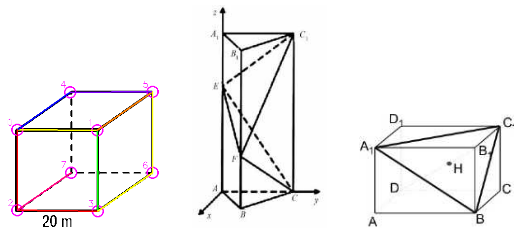

(a) (b) (c)

Figure 5: 3 Types of unnecessary edges. (a) type 1. (b) type 2. (c) type 3.

ment. Finally, the vertices of the sketch graph are obtained by merging the end points that are very close to each other, and the edges of the sketch graph are obtained according to the line segments. As shown in Figure 3(d), the graph vertices are circled and labeled by Arabic numbers, and the graph edges are drawn in different colors.

4.4 Unnecessary Edges Removal

Some of the extracted line segments are correct ones, but not useful or even harmful to the following reconstruction process. In order to successfully reconstruct the geometric object in the line drawing image, we use some heuristics to remove some of the vertices and edges from the obtained sketch graph as follows.

Type 1: Dangling Edges. In the extracted sketch graph, a vertex point whose degree equals to 1 is called a dangling point, and the corresponding edge is called the dangling edge. For example, the edge 2-7 in Figure 5(a) is a dangling one.

Type 2: Docking Edges. We call a line segment as "docking line segment" if one of its end points is at the middle of another line segment. And the corresponding edge is a docking edge. For example, in Figure 5(b), the line segments CE, CF, C_1E, and C_1F are docking ones.

Type 3: Diagonal Edges. The "diagonal line segment" is the one that connects the diagonal points of a parallelogram in the sketch. And the corresponding edge is a diagonal edge. As shown in Figure 5(c), the line segments A_1B, BC_1, and A_1C_1 are diagonal ones.

These unnecessary edges are excluded from the reconstruction process introduced in the next section.

5 3D MODEL SELECTION

After obtaining the sketch graph of the line drawing, we select some candidate 3D models with the similar graph structure from the pre-built 3D model database. The details will be introduced in the following subsections.

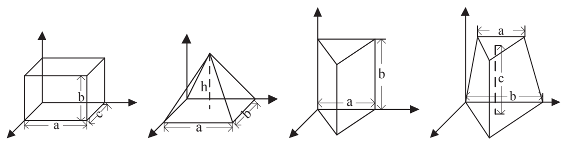

(a) (b) (c) (d)

Figure 6: Examples of the 3D models. (a) cuboid. (b) pyramid. (c) triangle-prism. (d) tetrahedron-frustum.

5.1 3D Model Database

In this work, a 3D model is represented as an undirected connected graph in the 3D space. Each vertex of the model has a 3D coordinate X_i, and the graph is represented by G_m. Moreover, a 3D model is controlled by a number of model parameters (denoted as set **A**), which represent the geometric attributes of the 3D model, such as width, height, depth. Some of the examples are shown in Figure 6. Figure 6(a) is a cuboid model. It has 3 parameters: $\mathbf{A}_{cuboid} = \{a, b, c\}$, where a, b, c are the width, height and length of the cuboid model respectively. For a 3D model M, we use a matrix which is composed by the elements of **A** to represent the 3D coordinates of the vertices, which is called the parametric matrix of the model and is denoted by V_M. For example, the parametric matrix of the cuboid is

$$V_{cuboid} = \begin{pmatrix} 0 & a & a & 0 & 0 & a & a & 0 \\ 0 & 0 & 0 & 0 & b & b & b & b \\ 0 & 0 & c & c & 0 & 0 & c & c \end{pmatrix}, \quad (1)$$

in which each column V_i is the 3D Euclidean coordinates of a vertex. Obviously, the parametric matrix always has 3 rows and the number of columns equals to the number of vertices.

We have totally defined 16 models to build the 3D model database, which can cover almost all the cases that appear in our experimental data set.

5.2 Matching the Sketch Graph within the 3D Model Database

We select the candidate models from the 3D model database based on sub-graph isomorphism. The sub-graph isomorphism is a graph matching technique to find a sub-graph in a given bigger graph G isomorphic to a given smaller graph H. We adopt the VF-2(Cordella et al., 2004) algorithm to accomplish our sub-graph isomorphism task.

We perform sub-graph isomorphism twice. In the first time, we take the sketch graph G_s as the bigger graph and the model graph G_m as the smaller graph; and in the second time, we conversely take G_m, G_s as the bigger graph and the smaller graph respectively.

The first time of sub-graph isomorphism is performed to handle the completely or over-completely extracted sketches. For example, Figure 3(d) illustrates the extracted sketch from a line drawing image of tetrahedron-frustum, in which the lines A_1B and A_1C are not contained in the model of the tetrahedron-frustum. We find the models whose number of vertices are equal to or smaller than that of the sketch, and are isomorphic to a sub-graph of the sketch. And among these models, only the ones with the largest number of vertices are selected as the candidate models. For the example shown in Figure 3(d), we first find 4 models – pyramid, tetrahedron, triangle-prism and tetrahedron-frustum, and finally select two models – the triangle-prism and the tetrahedron-frustum as the candidate models, which are shown in Figure 6(c) and 6(d).

During the process of the sketch extraction, some line segments may be not extracted or partially extracted, and thus the obtained sketch graph is usually incomplete. In order to deal with these cases, we perform the second time of sub-graph isomorphism – fix the 3D model G_m as the bigger graph, and find sub-graphs that are isomorphic to the sketch graph G_s in it. For example, Figure 5(a) shows an incomplete sketch extracted from a line drawing image of the cuboid. To be more specific, the two dashed lines (4-7 and 6-7) are completely missing. By applying the second time of sub-graph isomorphism, the correct candidate models (the cube and the cuboid et al) can still be selected.

The models selected by the two times of sub-graph isomorphism are all added to the list of candidate models, which will be used in the 3D reconstruction process.

6 3D RECONSTRUCTION

For each candidate 3D model, the reconstruction result is obtained by minimizing an objective function of the residuals between the vertices of the sketch and the 2D projections of the candidate model's vertices. And then, some bad reconstruction results are rejected. Finally, the optimal result that best fits the sketch is selected. The details of our reconstruction algorithm are introduced in the following subsections.

6.1 Recovery of Each Candidate Model

After a sub-graph isomorphism, we obtain some correspondence $\mathcal{C} = (\mathbf{X}^{\mathcal{C}}, \mathbf{x}^{\mathcal{C}})$ between the subsets of the vertices of the candidate model and the sketch graph, where $\mathbf{X}^{\mathcal{C}}$ and $\mathbf{x}^{\mathcal{C}}$ are subsets of $\mathbf{X}$ and $\mathbf{x}$ respectively, and $\mathcal{C}$ is a one-to-one correspondence relationship between $\mathbf{X}^{\mathcal{C}}$ and $\mathbf{x}^{\mathcal{C}}$. The coordinates of the subset $\mathbf{X}^{\mathcal{C}}$ are $\mathbf{X}^{\mathcal{C}} = \{X_{i_1}, X_{i_2}, \ldots, X_{i_{\mathcal{C}}}\}$, where i_k is the sub-indices of $\mathbf{X}$, and the coordinates of the subset $\mathbf{x}^{\mathcal{C}}$ are $\mathbf{x}^{\mathcal{C}} = \{x_{j_1}, x_{j_2}, \ldots, x_{j_{\mathcal{C}}}\}$, where j_k is the sub-indices of $\mathbf{x}$.

For each candidate model, the 3D reconstruction process of our method aims to find an instance of it whose 2D projection can best fit the sketch. To be more specific, our target is to optimize an objective function that minimizes the coordinate residuals between the matched vertices of the sketch and the candidate model. The objective function is the *projection error*, which is given by

$$f = \sum_{k=1}^{n_{\mathcal{C}}} \left\| K(RV_{i_k} + \mathbf{t}) - x_{j_k} \right\|^2, \tag{2}$$

where $n_{\mathcal{C}}$ is the number of corresponding pairs of the vertices; $K = \begin{pmatrix} 1 & 0 & 0 \\ 0 & 1 & 0 \end{pmatrix}$ is the parallel projection matrix, R is the rotation matrix, $\mathbf{t}$ is the translation vector, i_k and j_k are the indices of the corresponding vertices of the sketch and the model, V_{i_k} is the i_k-th column of the parametric matrix V, and x_{j_k} is the 2D coordinate of the j_k-th vertex of the sketch. The optimal solution is found by solving the following problem

$$\begin{gathered} \tilde{\mathbf{A}}, \tilde{R}, \tilde{\mathbf{t}} = \arg\min \sum_{k=1}^{n_{\mathcal{C}}} \left\| K(RV_{i_k} + \mathbf{t}) - x_{j_k} \right\|^2 \\ \text{subject to} : R^T R = I, \end{gathered} \tag{3}$$

where $\tilde{\mathbf{A}}$ is the optimal geometric parameters of the model, $\tilde{R}$ is the optimal rotation matrix, and $\tilde{\mathbf{t}}$ is the optimal translation vector.

The objective function is a quadratic function with an orthogonal constraint. We use the algorithm in (Xue et al., 2012) to solve the problem in (3).

6.2 Optimal Reconstruction Result Selection

For each candidate model, we obtain an reconstruction result by solving the objective function in (3). We further select the best result among these reconstruction results. The selection process is introduced as follows.

First, the result with large projection error should be rejected, that is, if the projection error $f > \delta$, the

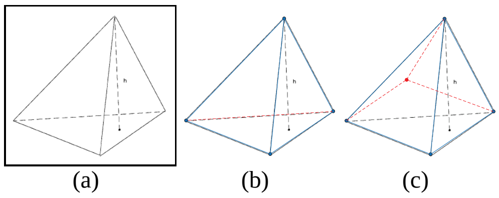
Figure 7: Example of pixel level validation. (a) a line drawing image contains a tetrahedron. (b) tetrahedron model with a missing line (red dashed line). (c) pyramid model with missing lines.

result should be directly rejected, where δ is an empirically set threshold (in this work, we set δ to 90.0).

Second, for the candidate models selected by the second time of sub-graph isomorphism, there exists some missing vertices and missing lines. For example, in Figure 7(a) (the vertical line inside the tetrahedron has been removed as it's a dangling line), the dashed line of the tetrahedron is missing due to failure of the sketch extraction step. Two candidate models are selected by the second time of sub-graph isomorphism: the tetrahedron and the pyramid, as shown in Figure 7(b) and 7(c) respectively. The tetrahedron model's missing line accurately overlaps with the dashed line in the image, while the pyramid model's missing lines do not hit any line in the image. Although the projection errors of the two models are exactly the same, we can select a better model by the "pixel validation": for each candidate model's reconstruction result, the "pixel vote" – the count of the foreground pixels that the missing lines of the reconstructed instance of the model pass through is collected. We look for the pixels on both sides of the missing lines at a small range, for tolerance of some coordinate inaccuracies. If a candidate model's pixel vote is significantly smaller than the others, it should be rejected.

Third, if two candidate models' projection error are nearly the same, we reject the one with a larger parameter set **A**, since it's a more complex model than the other one. We want to select the model as simple as possible, in order to solve the over-fit issue.

Finally, if there are still multiple candidate models, we choose the one with the smallest projection error as the final selected model.

The optimal reconstruction algorithm is shown in algorithm 2.

7 EXPERIMENT

We implement our algorithm in C++, and also develop a graphical application both on PC and mobile phone to demonstrate our method. As illustrated in our demo, with this graphical application, user first loads a PDF file and selects an rectangular area of 3D geometry illustration from some pages; and after the system processing, the reconstruction result is shown in a pop up window. User can zoom and drag to rotate the reconstructed object, as if it's immersed in a 3D space. No parameter setting is required for input; and the whole process usually only takes 1-10 seconds.

Algorithm 2 : 3D reconstruction from extracted sketch.

```
Input:
    extracted sketch graph $G_s$, candidate models $\{M_k\}$;
Output:
    the reconstructed 3D object;
1: For each candidate model $M_k$, solve the minimization problem in (3) by using algorithm in (Xue et al., 2012). Let $f_k$ denote the projection error, $p_k$ denotes the pixel vote, and $\mathbf{A}_k$ denotes the parameters set.
2: Find the candidate model with the highest pixel vote. Let $\hat{p}$ denote the highest pixel vote.
3: From the candidate models, remove the ones whose $f_k > \delta$.
4: If one candidate model is generated by the second time of sub-graph isomorphism, and its pixel vote $p_k < 0.1 * \hat{p}$, remove it.
5: Keep the candidate models whose parameters set $\mathbf{A}_k$ has the smallest number of parameters, remove all the others.
6: If there are still more than one candidate models, remove all except the one with the smallest projection error $f_k$.
7: With the only one left model and it's parameters, Output $RV + \mathbf{t}$ as the final reconstructed 3D object.
```

We collected over 40 PDF documents from the internet (including books, papers, teaching materials, slide shows and other types of documents), and captured 303 line drawing images from them. Our algorithm is tested over these line drawing images, and some examples of the reconstruction results are shown in Figure 8.

Evaluation. In the most related work of E3D (Xue et al., 2012), the authors use the RMSA (root mean squares of differences of angles) and the RMSE (root mean squares of differences of Euclidean distances) metrics to evaluate the reconstruction accuracy. However, we found these metrics not suitable for our case. The reasons can be described as below. First, the line drawings used in E3D are manually crafted in a CAD

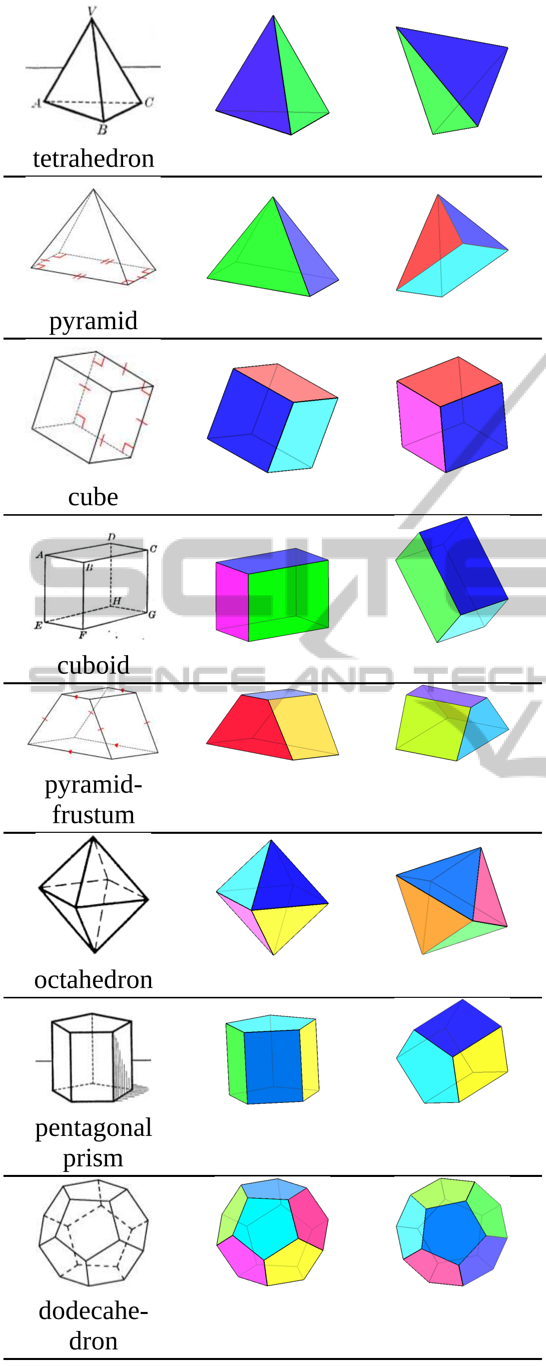

Figure 8: Examples of reconstruction results.The first column is the input line drawing image and the name of the 3D model. The second column is the reconstructed object from original angle of view. The third column is the object viewed from different angles.

software, so the ground truth is precisely known; while our input data is just the line drawing image. Second, for the applications such as mobile reading and learning, users tend to care about whether the reconstruction result is the right 3D object illustrated in the original line drawing image, rather than caring about how close the reconstructed angles and points are to the original line drawing. For these reasons, we use a simple metric – the matching accuracy to evaluate the proposed method and E3D. Let **F** denote the test image set, and $\mathbf{F}_{correct}$ denotes the set of correctly matched images, then the matching accuracy is defined as $f_a = \frac{|\mathbf{F}_{correct}|}{|\mathbf{F}|}$.

Table 1 compares the results of our method and E3D on our testing dataset. As we can see that the matching accuracy of our method is significantly higher than that of E3D. The reason why E3D performs so poorly is that, as we have known, it can only handle complete sketches while our method can also handle incomplete or over-complete sketches. And in our experiment, we find that, for most of the testing line drawing images, the extracted sketch is inaccurate (i.e., incomplete or over-complete). Therefore, our method performs much better than E3D.

Table 1: Comparison between our method and E3D.

Method	Correct match	Incorrect match	Accuracy
E3D	42	261	13.9%
Ours	221	82	72.9%

We can also extend our method to the natural images as shown in Figure 9. Given an input image, we first detect the straight lines in it as in Figure 9(b), and then extract the sketch using the straight lines as in Figure 9(c). Note that in this example, the extracted sketch is incomplete, and the hidden side of the object is invisible. Then the 3D geometric object in the image is reconstructed. We paste the textures in the image onto the faces of the box, as shown in Figure 9(d) and Figure 9(e). The whole process is done automatically, as opposed to the real image modeling example shown in E3D. They need the user to manually sketch along the edges of the object, and both the visible and invisible edges must be drawn in the sketch.

Failure Analysis. Most failure cases happen when there are both undetected and over-detected edges. For example, the oblique-pyramid in Figure 10(a) is mistakenly reconstructed as a tetrahedron in Figure 10(c). From the sketch in Figure 10(b), we can see that the edge `CD` fails to be detected, and there are some extra edges. Most extra edges like the axis and the edge `AF` has been removed by the heuristics we use, but the edge `AC` is not removed since the edge `CD` is not detected (thus the "diagonal heuristic" does not apply). Finally, we end up getting only wrong candidate models from the first round of sub-graph isomor-

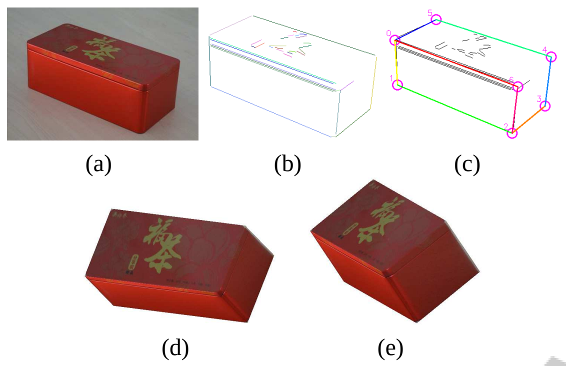

Figure 9: Example of modeling from natural image. (a) an input image. (b) straight lines detection. (c) sketch extraction. (d)(e) reconstructed 3D object in two different views.

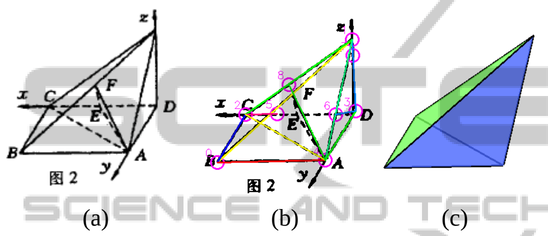

Figure 10: An example of failure case. (a) input image. (b) extracted sketch. (c) reconstruction result.

phism matching, and therefore it's impossible to get the correct reconstruction result.

Other failure cases include over-fitted model being taken, edges being too complicated to be reconstructed, et al. But these are only occasional cases. If we fine tune the algorithm to fit these occasional cases, the whole matching accuracy would decline.

8 CONCLUSION AND FUTURE WORKS

We have proposed a robust method to reconstruct 3D geometric object from single line drawing image. Solid and dashed straight line segments are first extracted from the image and further represented as an 2D undirected connected graph, namely, the sketch. Then, candidate models from a pre-built 3D model database are selected through two rounds of subgraph isomorphism. Furthermore, for each candidate model, reconstruction result is obtained by minimizing a cost function of residuals between the vertices of the sketch and the 2D projections of the corresponding vertices of the candidate model. Finally, some bad reconstruction results are rejected and the optimal result that best fits the sketch is outputted. The proposed method is tested on 303 line drawing images and the experimental results demonstrate that: (1) it can successfully reconstruct the solid geometric object from single line drawing image; (2) it achieves significantly higher matching accuracy than the state-of-the-art method E3D. Our future works include: (1) extracting line styles and labels to preserve the style of the input; (2) reconstruction of the curved objects, such as cylinders and spheres; (3) improving the reconstruction performance by taking syntax information into account; (4) reconstruction of complex line drawings, not limited to pre-built models in the model database.

ACKNOWLEDGEMENTS

We'd like to thank all the reviewers for providing encouraging and valuable comments to our work. This work is supported by National Natural Science Foundation of China under Grant 61300061 and Beijing Natural Science Foundation (4132033).

REFERENCES

Brown, E. and Wang, P. S. (1996). Three-dimensional object recovery from two-dimensional images: a new approach. In *Photonics East'96*, pages 138–147. International Society for Optics and Photonics.

Chen, Y., Liu, J., and Tang, X. (2007). A divide-and-conquer approach to 3d object reconstruction from line drawings. In *Computer Vision, 2007. ICCV 2007. IEEE 11th International Conference on*, pages 1–8. IEEE.

Cordella, L. P., Foggia, P., Sansone, C., and Vento, M. (2004). A (sub) graph isomorphism algorithm for matching large graphs. *Pattern Analysis and Machine Intelligence, IEEE Transactions on*, 26(10):1367–1372.

Cordier, F., Seo, H., Melkemi, M., and Sapidis, N. S. (2013). Inferring mirror symmetric 3d shapes from sketches. *Computer-Aided Design*, 45(2):301–311.

Hartigan, J. A. and Wong, M. A. (1979). Algorithm as 136: A k-means clustering algorithm. *Applied statistics*, pages 100–108.

Leclerc, Y. G. and Fischler, M. A. (1992). An optimization-based approach to the interpretation of single line drawings as 3d wire frames. *International Journal of Computer Vision*, 9(2):113–136.

Lee, Y. T. and Fang, F. (2011). 3d reconstruction of polyhedral objects from single parallel projections using cubic corner. *Computer-Aided Design*, 43(8):1025–1034.

Lee, Y. T. and Fang, F. (2012). A new hybrid method for 3d object recovery from 2d drawings and its validation against the cubic corner method and the optimisation-based method. *Computer-Aided Design*, 44(11):1090–1102.

Lipson, H. and Shpitalni, M. (1996). Optimization-based reconstruction of a 3d object from a single freehand line drawing. *Computer-Aided Design*, 28(8):651–663.

Liu, D., Wang, Y., Tang, Z., Li, L., and Gao, L. (2014). Automatic comic page image understanding based on edge segment analysis. In *Proc. SPIE 9021, Document Recognition and Retrieval XXI*, pages 90210J–90210J–12.

Liu, J., Cao, L., Li, Z., and Tang, X. (2008). Plane-based optimization for 3d object reconstruction from single line drawings. *Pattern Analysis and Machine Intelligence, IEEE Transactions on*, 30(2):315–327.

Liu, J., Chen, Y., and Tang, X. (2011). Decomposition of complex line drawings with hidden lines for 3d planar-faced manifold object reconstruction. *Pattern Analysis and Machine Intelligence, IEEE Transactions on*, 33(1):3–15.

Liu, J. and Lee, Y. T. (2001). Graph-based method for face identification from a single 2d line drawing. *Pattern Analysis and Machine Intelligence, IEEE Transactions on*, 23(10):1106–1119.

Liu, J., Lee, Y. T., and Cham, W.-K. (2002). Identifying faces in a 2d line drawing representing a manifold object. *Pattern Analysis and Machine Intelligence, IEEE Transactions on*, 24(12):1579–1593.

Liu, J. and Tang, X. (2005). Evolutionary search for faces from line drawings. *Pattern Analysis and Machine Intelligence, IEEE Transactions on*, 27(6):861–872.

Marill, T. (1991). Emulating the human interpretation of line-drawings as three-dimensional objects. *International Journal of Computer Vision*, 6(2):147–161.

Otsu, N. (1975). A threshold selection method from gray-level histograms. *Automatica*, 11(285-296):23–27.

Shoji, K., Kato, K., and Toyama, F. (2001). 3-d interpretation of single line drawings based on entropy minimization principle. In *Computer Vision and Pattern Recognition, 2001. CVPR 2001. Proceedings of the 2001 IEEE Computer Society Conference on*, volume 2, pages II–90. IEEE.

Shpitalni, M. and Lipson, H. (1996). Identification of faces in a 2d line drawing projection of a wireframe object. *Pattern Analysis and Machine Intelligence, IEEE Transactions on*, 18(10):1000–1012.

Tian, C., Masry, M., and Lipson, H. (2009). Physical sketching: Reconstruction and analysis of 3d objects from freehand sketches. *Computer-Aided Design*, 41(3):147–158.

Xue, T., Liu, J., and Tang, X. (2010). Object cut: Complex 3d object reconstruction through line drawing separation. In *Computer Vision and Pattern Recognition (CVPR), 2010 IEEE Conference on*, pages 1149–1156. IEEE.

Xue, T., Liu, J., and Tang, X. (2012). Example-based 3d object reconstruction from line drawings. In *Computer Vision and Pattern Recognition (CVPR), 2012 IEEE Conference on*, pages 302–309. IEEE.

Yang, L., Liu, J., and Tang, X. (2013). Complex 3d general object reconstruction from line drawings. In *Computer Vision (ICCV), 2013 IEEE International Conference on*, pages 1433–1440.

Zou, C., Chen, S., Fu, H., and Liu, J. (2014a). Progressive 3d reconstruction of planar-faced manifold objects with drf-based line drawing decomposition. *Visualization and Computer Graphics, IEEE Transactions on*, PP(99):1–1.

Zou, C., Yang, H., and Liu, J. (2014b). Separation of line drawings based on split faces for 3d object reconstruction. In *Computer Vision and Pattern Recognition (CVPR), 2014 IEEE Conference on*, pages 692–699.